

Emerging Topics in Statistics and Biostatistics

Andriëtte Bekker  
(Din) Ding-Geng Chen  
Johannes T. Ferreira  
*Editors*

# Computational and Methodological Statistics and Biostatistics

Contemporary Essays in Advancement



Springer

# Applications of Spatial Statistics in Poverty Alleviation in China



Yong Ge, Shan Hu, and Mengxiao Liu

**Abstract** China is the most populous country in the world, especially a large number of impoverished people concentrated in rural area. The uneven distribution of impoverished people in China has made it necessary to investigate its spatial patterns and driving forces. In this chapter, several methods of spatial statistics that have been employed to poverty issues analysis were reviewed. These methods were mainly used to investigate the driving forces, spatial patterns, and spatial temporal changes of poverty. Three case studies of China were then conducted to provide the detail illustrations of the application of the methods.

## 1 Background

Poverty is a common challenge that accompanies the progress of human society. The first goal of the sustainable development goals (SDGs) proposed by the United Nations is to end poverty in all its forms everywhere by 2030 (United Nations 2015a). China, a developing country with a large rural poor population, has made great efforts to improve development in poor areas over the past decades and has seen tremendous improvements (Information Office of the State Council 2011). Despite this great achievement, there are some issues such as poverty-returning phenomenon, developmental contradiction between economy and ecology, and regional development disparities that also need to be addressed (Wang et al. 2014). In addition, the distribution of the impoverished people in China is uneven, which makes it necessary to investigate spatial patterns and driving forces to better support effective poverty reduction measures.

---

Y. Ge (✉) · S. Hu · M. Liu

State Key Laboratory of Resources and Environmental Information System, Institute of Geographical Sciences and Natural Resources Research, Chinese Academy of Sciences, Beijing, China

e-mail: [gey@lreis.ac.cn](mailto:gey@lreis.ac.cn)

© Springer Nature Switzerland AG 2020

A. Bekker et al. (eds.), *Computational and Methodological Statistics and Biostatistics*, Emerging Topics in Statistics and Biostatistics,  
[https://doi.org/10.1007/978-3-030-42196-0\\_16](https://doi.org/10.1007/978-3-030-42196-0_16)

367

### ***1.1 Poverty in China: Responses, Achievements, and Problems***

China has made great efforts to reduce the rural poor population over the past decades. Various policies and measures have been implemented with positive results. Despite this, China still faces several challenges in poverty alleviation.

Since the reform and opening up in 1978, China has entered a critical period of urbanization and industrialization, leading to fast economic development, a considerable increase in living standards, and an unprecedented decline in poverty (Wang et al. 2014). China has made numerous efforts to accelerate development in poverty-stricken areas. Specifically, it has implemented the Seven-Year Priority Poverty Reduction Program (1994–2000), Outline for Poverty Reduction and Development of China's Rural Areas (2001–2010), Outline for Development-Oriented Poverty Reduction for China's Rural Areas (2011–2020), and Targeted Poverty Reduction Strategy (2013) (Zuo 2016; The State Council 2011). These policies and programs have significantly promoted development in poverty-stricken areas and helped thousands of people out of poverty.

Benefitting from various measures, China became the first developing country in the world to achieve the poverty reduction target set by the Millennium Development Goals of halving the proportion of people whose income is less than \$1.25 per day. Owing to China's progress, the extreme poverty rate in eastern Asia has dropped from 61% in 1990 to only 4% in 2015 (United Nations 2015b). Based on the current national poverty line, CNY 2300 per capita annual net income, the poverty headcount ratio in China has fallen from 97.5% in 1978 to 1.7% in 2018 (Department of Household Surveys, National Bureau of Statistics of China 2018; National Bureau of Statistics 2019). On top of that, housing, education, transportation, and medical care have all seen significant improvements. In particular, the implementation of the Entire-Village Advancement, which covers basic farmland, drinking water, roads, social undertakings, and other aspects that affect impoverished villages, has significantly improved the living standard in rural areas (Li et al. 2016; Zhou et al. 2018; Liu et al. 2018).

Owing to a poor economic foundation and restriction of natural environment conditions, central and western China are still developing slowly, and regional disparities, especially rural–urban disparities, are increasing (Dollar 2007). At the end of 2018, there were 16.60 million people living below the national poverty line (Li et al. 2016). Moreover, a number of people who returned to poverty started to appear, owing to such factors as disasters, illness, disability, and school costs (Zhou et al. 2018). Meanwhile, a strong connection between poverty-stricken areas and ecologically protected areas has led to a contradiction between a balanced development of socioeconomic and ecological conditions (Ouyang et al. 2016; Xu et al. 2017). Regional development disparities and inequality has also put pressure on China's poverty reduction efforts.

1.2 Spatial Characteristics of Poverty in China

China’s poverty-stricken areas are mainly concentrated in central and western China, most of which are hilly and mountain areas.

The distribution of poverty-stricken areas in China has an obvious spatial agglomeration feature. Liu et al. (2017) found that impoverished people mainly concentrate in the remote deep mountain areas, border areas, and minority areas of central and western China, and they gradually gather towards the southwestern region. After the promulgation of the Outline for Development-Oriented Poverty Reduction for China’s Rural Area (2011–2020) in 2011, the Chinese government identified 14 poverty-stricken areas as the main battleground for the new round of poverty reduction and development efforts. Figure 1 shows that poverty-stricken areas are mainly located in Western and Central China. The 14 poverty-stricken areas contain 680 counties and cover approximately one third of China, with mountainous and hilly areas accounting for 86.8% of the land (Zuo 2016).

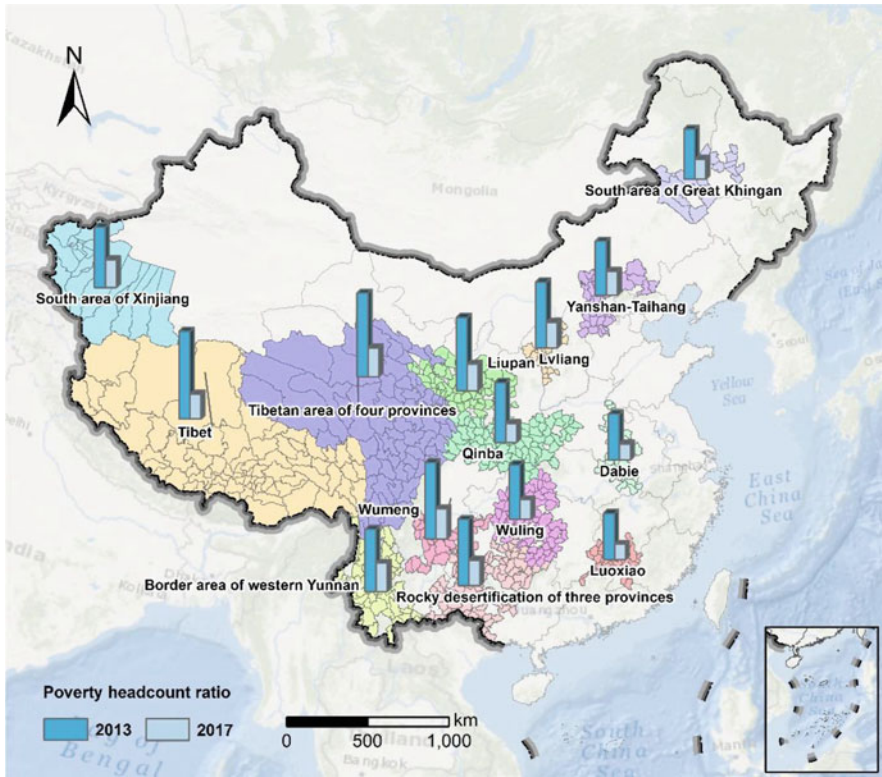


Fig. 1 Fourteen continuously poverty-stricken areas and their poverty headcount ratio in 2013 and 2017, respectively

The uneven distribution of China's rural poor population has made it necessary to explore the spatial pattern and their main causes. The geography of poverty has been developing rapidly in China since the vigorous carrying out of poverty reduction actions. A large number of spatial statistical methods were employed to explore geographical distribution patterns (Liu et al. 2017; Chen and Ge 2015), causes of poverty (Ren et al. 2017), geographical identification of poverty (Liu and Xu 2016), spatial-temporal changes of poverty (Li et al. 2015), poverty alleviation effectiveness assessment (Ge et al. 2017), and relationships between poverty and geographical elements (Okwia et al. 2007). The spatial temporal patterns and driving forces of poverty are revealed by spatial analysis and poverty mapping, which can support effective policies for poverty reduction and sustainable development in poverty-stricken areas.

## 2 Applications of Spatial Statistical Methods on Poverty

Evidences from various theoretical analysis of poverty have shown that poverty has spatial attributes (Bird 2019; Jalan and Ravallion 1997). Spatial statistical methods provide diverse tools for geographical poverty identification, spatial disparities analysis, and spatial-temporal analysis.

### 2.1 Datasets

Poverty headcount ratio is the percentage of people living below the poverty line. The poverty headcount ratio is usually used as a response variable in poverty related spatial statistical analysis. The potential explanatory variables were selected from the aspects of income, education, healthcare, housing, and infrastructure for a region. Meanwhile, the spatially referenced environmental indicators such as topography, land cover and land use, access to public services were also selected as potential explanatory variables.

Poverty was initially treated as an economic phenomenon and was usually measured by the amount of money a person had to meet certain basic needs (Sen 1976; Atkinson 1987). Amartya Sen put forward the concept of capability poverty in his book *Development as Freedom* (Sen 2001). This revolutionary leap helped many researchers understand poverty from different perspectives. Now, poverty is identified as a multidimensional phenomenon that includes various elements, such as economic shortage, social exclusion, and vulnerability (Alkire and Foster 2011; Satya and Chakravarty 2006). Based on these varying perspectives of understanding poverty, there are also multiple ways to measure poverty. From measuring just income to including other factors such as health, education, and social services, the measurement of poverty has gradually extended to appraise the sustainable livelihoods of the poor population (Alkire and Fang 2018). Income poverty, the

**Table 1** Part of the county level socioeconomic data this chapter used

County name	Poverty headcount ratio (%)	Teachers per 10,000 persons (per-sons/10,000)	Number of beds utilized in health care institutions per 10,000 persons (persons/10,000)	Disposable income of rural household (CNY)
Kangding	12.10	111.27	91.88	6554.17
Luding	16.30	107.21	30.76	5772.54
Danba	15.44	114.32	36.79	6356.66
Jiulong	14.84	93.56	29.84	7004.28
Yajiang	18.65	86.96	27.00	5374.37
Daofu	19.89	76.59	30.35	5047.35
Luhuo	19.86	97.92	41.36	4989.93
Ganzi	20.85	86.60	41.50	5161.84
Xinlong	19.70	88.28	23.05	5022.94
Dege	23.52	72.57	15.00	4884.12

human development index (HDI), and the multidimensional poverty index (MPI) are all widely used to measure global poverty (Wang 2012).

Income poverty is the most widely used tool to measure poverty. The World Bank built bridges to global poverty measurement. The \$1.90 per day is the new international poverty line determined by the World Bank in 2015 (The World Bank 2018). The current national poverty line in China is CNY 2300 per capita annual net income (Department of Household Surveys, National Bureau of Statistics of China 2018). The population living below the poverty line are identified as impoverished people. The poverty headcount ratio is the proportion of the impoverished people to the total population. In this chapter, the poverty headcount ratio is used as a response variable. Table 1 provides part of the poverty headcount ratio at the county level of China in 2013.

The HDI and MPI are looks beyond the income to measure poverty. HDI is a summary measure of average achievement in three dimensions of human development for a country: a long and healthy life, being knowledgeable, and have a decent standard of living (UNDP 2010). While MPI emphasizes multiple deprivations at the household and individual level in health, education and standard of living. The specific indicators of MPI include nutrition, child mortality, years of schooling, school attendance, cooking fuel, sanitation, drinking water, electricity, housing, and assets (Alkire and Foster 2011). These widely recognized literatures provide the basis for indicators selection. In this chapter, we selected county-level indicators from the aspects of regional economic, infrastructure, housing, healthcare, education, and medical care, as shown in Table 2.

Evidences from poverty mapping of China shows that the distribution of poverty is not homogenous (Zhang et al. 2014). From the perspective of geography, the heterogeneities are largely caused by the disparities in geographical conditions such as resource endowment, ecological environment, access to public services, and regional culture and polices (Zhou and Liu 2019). Existing researches have shown

**Table 2** Lists of the socioeconomic indicators

Contents	Indicators
Education	Teachers per 10,000 persons (persons/10,000)
	Ratio of expenditure on science and education to GDP (%)
Health care	Medical technical personnel in health care institutions per 10,000 persons (persons/10,000)
	Number of beds utilized in health care institutions per 10,000 persons (persons/10,000)
Living standard	Engel’s coefficient (%)
Infrastructure	Popularization rate of tap water (%)
	Ratio of administrative villages that can be reached by road (%)
Housing	Per-capita living space (m <sup>2</sup> per capita)
Medical care	New Rural Co-operative Medical System participants as a proportion of total population (%)
Income	Disposable income of rural household (CNY)

**Table 3** Lists of the environmental indicators

contents	Indicators
Environmental	Mean elevation
	Standard deviation of elevation
	Mean slope
	Standard deviation of slope
	Proportion of cropland
	Proportion of forest
	Proportion of grassland
	Proportion of built-up land
	Road density (km/km <sup>2</sup> )

that topography, elevation, slope, land use types are all closely related to poverty (Zhou and Liu 2019; Cheng et al. 2018; Watmough et al. 2019). This chapter has also selected few Geographical Information System-based indicators as explanatory variables to investigate the relationship between environmental factors and poverty, as shown in Table 3.

The sources of socioeconomic data mainly included: (1) the socioeconomic data from 2010 to 2016 in Ganzi collected from the statistical yearbook of Ganzi Tibetan Autonomous Prefecture (2011–2017) and the statistical bulletins of the national economic and social development from 2010 to 2016 in Ganzi Tibetan Autonomous Prefecture; (2) The impoverished population data in 2013 were provided by the State Council Leading Group Office of Poverty Alleviation and Development.

The sources of Geographical Information System-based data mainly included: (1) Elevation data was obtained from ASTER GDEM (Advanced Spaceborne Thermal Emission and Reflection Radiometer Global Digital Elevation Model) with resolution of 30 × 30 m., which was downloaded from Geospatial Data Cloud Web (<http://www.gscloud.cn/>). (2) Slope data were extracted from the DEM. (3) The land

cover and land use was collected from China's Land-Use/cover Datasets (CLUDs), which are provided by Resources and Environmental Data CloudPlatform(resdc.cn) with the spatial resolution of  $1 \times 1$  km. (4) Road data was obtained from National Catalogue Service For Geographic Information with the scale of 1:250000.

## 2.2 Causes of Poverty

Identifying the determinants of poverty is crucial for making effective poverty reduction policies in a region. This part introduces three widely employed spatial statistic methods for causes of poverty analysis: Geographical detector, Spatial regression, and Geographically Weighted Regression.

The geographical detector was developed by Wang et al. (2010), and was first applied in public health risk assessment. The core concept of the geographic detector is based on the assumption that if an explanatory variable has an important effect on the response variable, then the spatial distribution of the explanatory variable and response variable will be similar (Wang et al. 2010, 2016). All the results are based on the geographical detector q-statistic, which is defined as:

$$q = 1 - \frac{SSW}{SST} \quad (2-1)$$

$$SSW = \sum_{h=1}^L N_h \sigma_h^2 \quad SST = N \sigma^2 \quad (2-2)$$

$h(1, 2, \dots, L)$  is the strata of the explanatory variable (X) or response variable (Y).  $N$  and  $\sigma^2$  are the number of units and the variance of Y in the study area, respectively.  $N_h$  and  $\sigma_h^2$  are the number of units and the variance of Y in stratum  $h$ , respectively. SSW and SST are the within sum of squares and total sum of squares, respectively. The value of the q-statistic is within [0,1]. When response variable Y is stratified by Y itself, then the larger the q value, the more obvious the spatial stratified heterogeneity of Y. When Y is stratified by X, a larger  $q$  value indicates that X could explain more of Y, especially when  $q = 1$  indicates that Y is completely determined by X (Wang et al. 2016). Based on the geographical detector, Liu and Li (2017) investigated the spatial heterogeneity mechanism of poverty in Fuping County, China. They denoted the poverty headcount ratio at village level as the response variable, and chose slope, elevation, per capita cropland, and distance to the town as the explanatory variables.

Classic ordinary least squares (OLS) regression assumes that the observations of explanatory variables are independent from each other and always in a normal distribution, as well as the error term (Anselin 2002; Anselin and Rey 1991). Therefore, if there is spatial autocorrelation in the data, the assumptions are violated. The regression models that take spatial autocorrelation into consideration are called



spatial regression models. Spatial autocorrelation can be detected by the global and local autocorrelation model, including Geary's C, G statistic, Moran's I index, and the local indicator of spatial association (LISA) (Anselin 1995; Getis 1994). The spatial regression model includes two main variations: the spatial lag model and the spatial error model. Spatial-lag model applies to a situation in which the response variable in one region is affected by the response variable in nearby regions; Spatial error model applies to a situation in which the error for the model in one region is correlated with the error terms in its neighboring regions (Anselin 2001; Paul Elhorst 2014). Paul O. Okwia et al. (2007) employed the spatial regression model to investigate how and which spatial factors are related to poverty and how much of the variation in poverty incidence can be explained by environmental factors in rural Kenya.

$$\text{Spatial lag model : } y_i = \lambda \sum_{j \neq i} w_{ij} y_j + \beta X_j + \varepsilon_j \quad (2-3)$$

$$\text{Spatial error model : } y_i = \beta X_j + \lambda \sum_{j \neq i} w_{ij} y_j \varepsilon_j + \varepsilon_j \quad (2-4)$$

$y_i$  is the response variable for region  $i$ ;  $\lambda$  is the spatial autoregressive coefficient;  $w_{ij}$  is the spatial weight reflecting the proximity of  $i$  and  $j$ ;  $y_j$  is the response variable for region  $j$ ;  $\beta$  is a vector of coefficients;  $X_j$  is a matrix of explanatory variables;  $\varepsilon_j$  is the error term (Paul Elhorst 2014).

Geographically weighted regression (GWR) was proposed by Fotheringham et al., which allowed the relationships to vary over space (Fotheringham et al. 2002). GWR is a local version of spatial regression that runs a regression for each location instead of a single regression model for the whole study area (Zhang et al. 2011; Tu and Xia 2008). GWR is also popular in the spatial modeling of poverty for providing a method to assess the degree to which the relationship between the potential determinants and the poverty rate varies across space. Steven Deller employed GWR to analyze the spatial variation in the role of tourism and recreation in changing poverty rates (Deller 2010).

$$y_i = \beta_0(u_i, v_i) + \beta_1(u_i, v_i)x_{1i} \cdots + \beta_n(u_i, v_i)x_{ni} + \varepsilon_i \quad (2-5)$$

$y_i$  is the response variable for location  $i$ ;  $\beta_i$  are to be estimated at location  $i$  whose coordinates are given by the vector  $(u_i, v_i)$ . The regression model is calibrated for a location by combining all other available data points to which weights are applied according to a continuous distance-decay function. The decay function could be fixed (commonly the Gaussian function is adopted) or adaptive. The shape of the function, defined by the adaptive bandwidth, may vary depending on the density of data points in the immediate neighborhood of the regression point (Fotheringham et al. 2015).

### 2.3 Spatial Pattern of Poverty

The spatial patterns can be recognized as cluster, randomness, dispersed, and uniformity. Understanding the spatial patterns of poverty areas and poverty populations can help uncover the causes of poverty and effectively implement poverty reduction measurements.

The multi-distance spatial cluster based on Ripley's K is a method that can analyze spatial patterns of point data (Ripley 1977). It summarizes the objects clustering or objects dispersion over a range of distances, which can be used to investigate how the clustering or dispersion of objects changes from distances. Therefore, the starting distance and distance increment are needed for a multi-distance spatial cluster analysis. It calculates the average number of neighboring objects associated with each object in a given distance.

$$\hat{K}(d) = \frac{A}{n^2} \sum_{i=1}^n \sum_{j \neq i}^n w_{ij} I(d_{ij} < d). \quad (2-6)$$

$$\hat{L}(d) = \sqrt{\hat{K}(d)/\pi} - d \quad (2-7)$$

$A$  is the area of observed points;  $n$  is the number of points;  $w_{ij}$  is an edge-correction term to remove the bias;  $I(d_{ij} < d)$  is an indicator function that takes the value 1 when distance  $d_{ij}$  between point  $i$  and  $j$  is less than  $d$ .  $\hat{L}_0(d)$  is compared with expected value  $\hat{L}_e(d)$  for a random sample of points from a complete spatial randomness pattern. If  $\hat{L}_0(d) - \hat{L}_e(d) > 0$ , the pattern of observed points at a distance scale  $d$  is cluster. If  $\hat{L}_0(d) - \hat{L}_e(d) < 0$ , the pattern is dispersed. If  $\hat{L}_0(d) - \hat{L}_e(d) = 0$ , the pattern is randomness.

The average nearest neighbor (ANN) ratio measures the distance between each object's centroid and its nearest neighbor's centroid location first, and then it averages all the nearest neighbor distances (Ebdon 1985). If the average nearest neighbor distance is less than the average for a hypothetical random distribution, the distribution of the objects is recognized as clustering. Conversely, if the average nearest distance is greater than the average for a hypothetical random distribution, the distribution of the objects is recognized as dispersed. Then, the average nearest neighbor ratio is calculated by the observed average distance and divided by the expected average distance. If the value of the average nearest neighbor ratio is less than 1, then it indicates a clustering pattern, while greater than 1 indicates a dispersed pattern.

$$ANN = \frac{\overline{D_0}}{\overline{D_e}} \quad (2-8)$$

$$\overline{D_0} = n^{-1} \sum_{i=1}^n d_i \quad (2-9)$$

$$\overline{D_e} = 0.5(n/A)^{-0.5} \tag{2-10}$$

$\overline{D_0}$  is the mean distance between each observed point and its nearest neighbor;  $\overline{D_e}$  is the expected mean distance from the points given in complete spatial randomness pattern;  $d_i$  is the distance between point  $i$  and its nearest neighbor;  $A$  is the area of observed points;  $n$  is the number of points.

Chen and Ge (2015) employed the multi-distance spatial cluster method to analyze the spatial pattern variation characteristics of 191,537 administrative villages in the 14 poverty-stricken areas of China. Meanwhile, they estimated the spatial pattern of villages in each county by using the average nearest neighbor ratio. The spatial pattern of the villages within each county is shown in Fig. 2. They found that village-clustered counties are the Tibet area and Tibetan ethnic areas in Sichuan, Yunnan, Gansu, and Qinghai provinces. Meanwhile, with the increase of distance, different

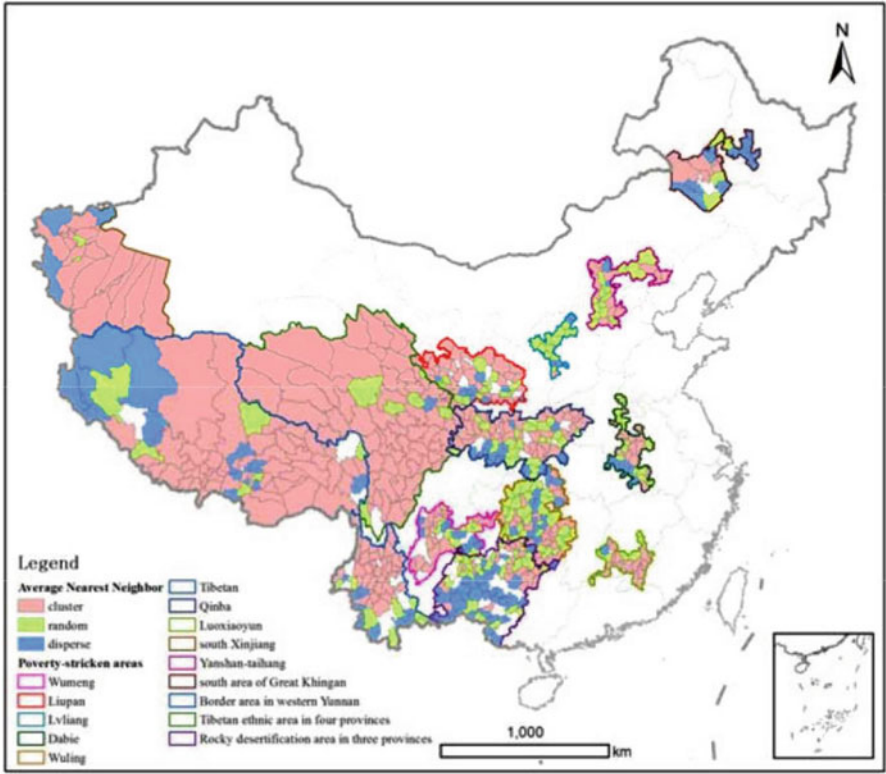


**Fig. 2** Point pattern of villages within each county in the 14 poverty-stricken areas of China (Source: Yuehong Chen, Yong Ge. Spatial point pattern analysis on the villages in China’s poverty-stricken areas. *Procedia Environment Sciences* 27(2015) 98–105)

poverty-stricken areas presented different distribution characteristics. Some areas showed spatial aggregation with distance, while others showed a pattern from aggregation to dispersion.

LISA is also used to investigate the spatial pattern of poverty areas or poor populations. The local Moran's I was used to obtain cluster maps of local indicators of spatial association that included statistically significant clusters of high values (high–high), clusters of low values (low–low), outliers in which a high value is surrounded primarily by low values (high–low), and outliers in which a low value is surrounded by high values (low–high) (Anselin 1995). Various researches use LISA to obtain the spatial pattern of the poverty rate, MPI index, and other comprehensive assessment indices at a county or village level.

$$I_i = \frac{\sum_{i=1}^n \sum_{j=1}^n W_{ij} \times (x_i - \bar{x})(x_j - \bar{x})}{\frac{1}{n}(x_i - \bar{x})^2} \quad (2-11)$$

$I_i$  is the local Moran's I for region  $i$ ,  $x_i$  is the attribute of region  $i$ ,  $\bar{x}$  is the mean of the corresponding attribute,  $w_{ij}$  is the spatial weight between counties  $i$  and  $j$ , and  $n$  is the total number of regions.

## 2.4 Spatial-Temporal Analysis of Poverty

Poverty is changing in number and region. The proportion of people living on less than \$1.25 per day globally fell from 36% in 1990 to 12% in 2015. While this achievement has been experienced in south Asia and Latin America, the sub-Saharan Africa region still lags behind (United Nations 2015b). Under the background of an unprecedented execution of poverty reduction policies, China's poverty-stricken areas are experiencing great changes. It is necessary to analyze the spatial-temporal change of the distribution of poor populations, causes of poverty, and economic-social-ecological conditions in China's poverty-stricken areas.

The most widely used and easiest way to explore the spatial-temporal change of poverty is to map the evaluation value of different times and compare them. However, if the observed time period is long and we want to investigate the continuous time series change pattern, then it will be time consuming and missing some information. Therefore, methods that can capture the change trajectories and spatial pattern is needed. The Bayesian hierarchical model (BHM) is used in the space-time analysis of burglary risk and incidence of poverty (Li et al. 2014; Sparks and Campbell 2013). Bayesian inferences combine the data with additional prior information to obtain more stable results. BHM considers the spatial and temporal correlation through prior information. BHM can quantitatively estimate the overall spatial distribution pattern, overall change trend, and local change trend in the spatial-temporal process (Haining 1990). It can also be employed to analyze the

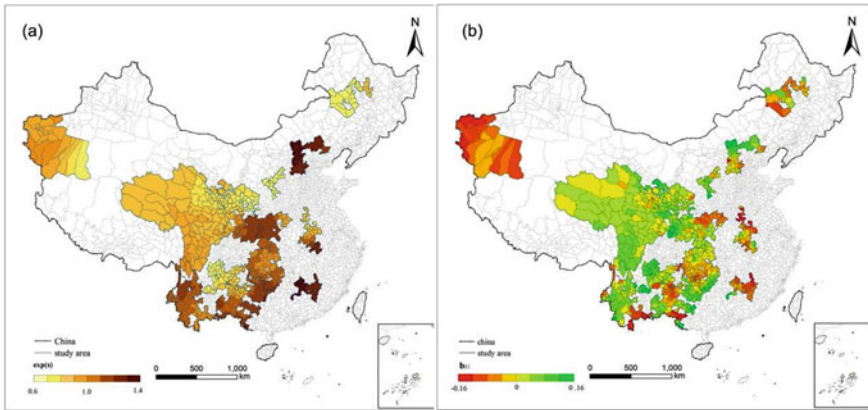


**Fig. 3** (a) Estimates from model: common spatial component (posterior medians of  $\exp(S_i)$ ); (b) Estimate from model: local trends' departure from overall trend (Source: Yong Ge, Yue Yuan, Shan Hu, Zhoupeng Ren, Yijin Wu. Space-time variability analysis of poverty alleviation performance in China's poverty-stricken areas. *Spatial Statistics* 21(2017) 460–474)

spatial-temporal change of poverty. Corey Sparks and Joey (2014) employed BHM to model and estimate the poverty rate in the United States at the county level. Ge et al. (2017) used BHM to assess the poverty reduction performance of China's poverty-stricken areas; they found a stable spatial pattern of higher effectiveness of poverty reduction in eastern China and lower in the western region, as shown in Fig. 3a. Meanwhile, for capturing spatial-temporal changes, the increasing trend of poverty reduction effectiveness presents a pattern of “high in the center, low in the east-west,” Fig. 3b, and the most poverty-stricken counties' development of poverty reduction effectiveness are consistent with the overall trend.

### 3 Case Studies for China

Based on the spatial statistical methods described in Sect. 2, this part conducted three case studies in China. In the first case, we analysis the spatial pattern of poverty headcount ratio of China's poverty-stricken areas by using LISA. The second case employed the GWR to explore the spatial nonstationary of the effect of geographic factors over the space in Hubei province of China. The third case first evaluate the living standard in Ganzi Tibetan Autonomous Prefecture from the aspects of housing, infrastructure, medical care, social security, and education based on the entropy weighting method and gray rational analysis. Then, the Bayesian hierarchical model was used to investigate the spatial-temporal changes of evaluated living standard index of each county in Ganzi from 2010 to 2016.

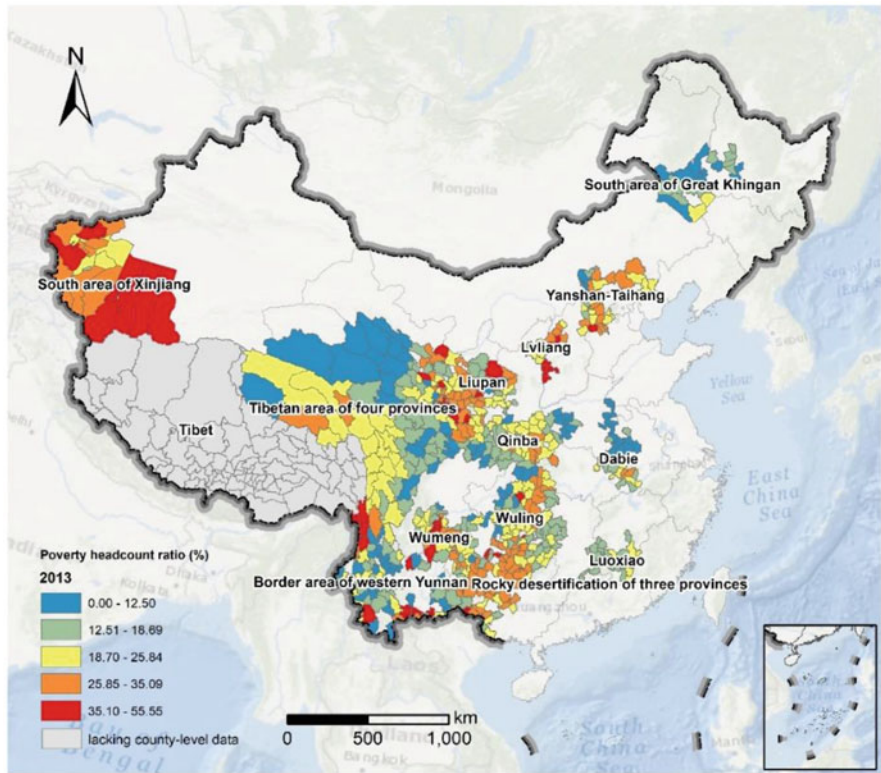


Fig. 4 The poverty headcount ratio of poverty-stricken counties in 2013

3.1 Spatial Pattern of Poverty Headcount Ratio

As it shows that in Fig. 1, China has identified 14 poverty-stricken areas as the new battleground of poverty reduction and development. Here we chose 13 of them, except Tibet area as it lacks county-level data, 601 counties in total to investigate the spatial pattern of poverty headcount ration in 2013. Figure 4 mapped the poverty headcount ration of poverty-stricken counties in 2013.

Local indicators of spatial association (LISA) was calculated by using the GeoDa software. Figure 5 shows the cluster maps of poverty headcount ratio for poverty-stricken areas. The counties that have high poverty rate mainly concentrated in South area of Xinjiang, most area of which is desert and Gobi. While the counties that have low poverty rate mainly located in Dabie area and South area of Great Khingan Great, both of which are national major grain producing areas.



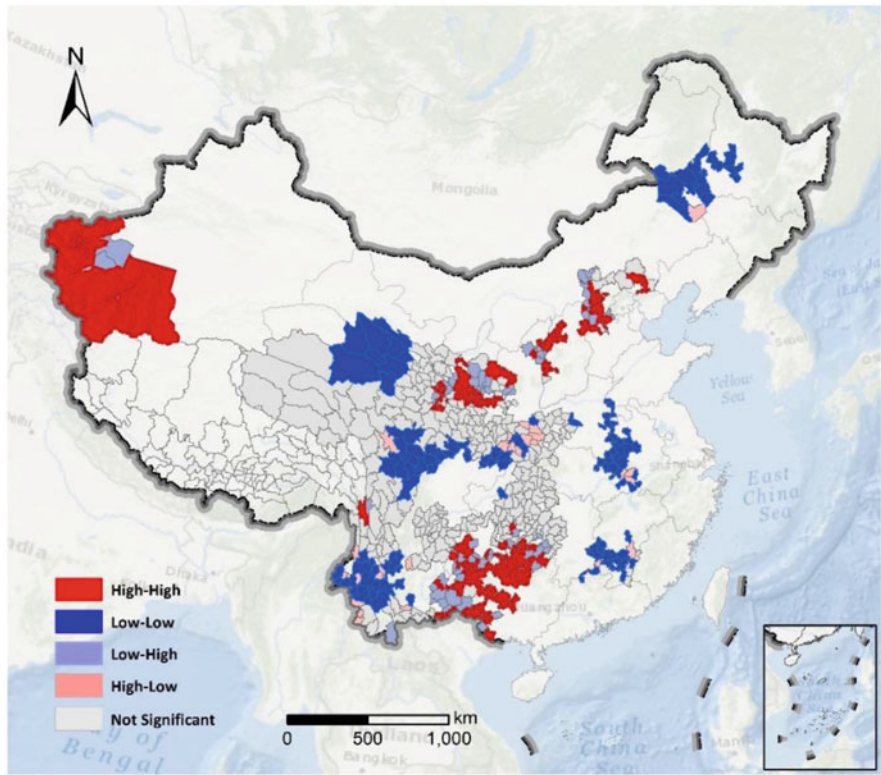


Fig. 5 Cluster maps for poverty headcount ratio in poverty-stricken areas

3.2 *Spatial Correlation Analysis: Case Study of Hubei Province in China*

Hubei province located in central China. The central and southern Hubei mainly belongs to Jiangnan Plain while the western and the peripheries are mountain areas.  $G_i^*$  was adopted to investigate the local spatial autocorrelation in Hubei province. The results shown in Fig. 6 suggested that a high-high cluster of Hubei province appeared in the west of Hubei province while a low-low cluster appeared in the surrounding areas of the capital city Wuhan. Poverty headcount ratio in Hubei province showed an obvious spatial pattern.

Some potential geographic factors contributing to poverty having available data and a narrow relevance were proposed as explanatory variables in this case. A total of 11 indicators were selected as the explanatory variables for the spatial regression analysis. The detailed description of the explanatory variables is presented in Table 3. The environment dimension includes topography and land resources. The

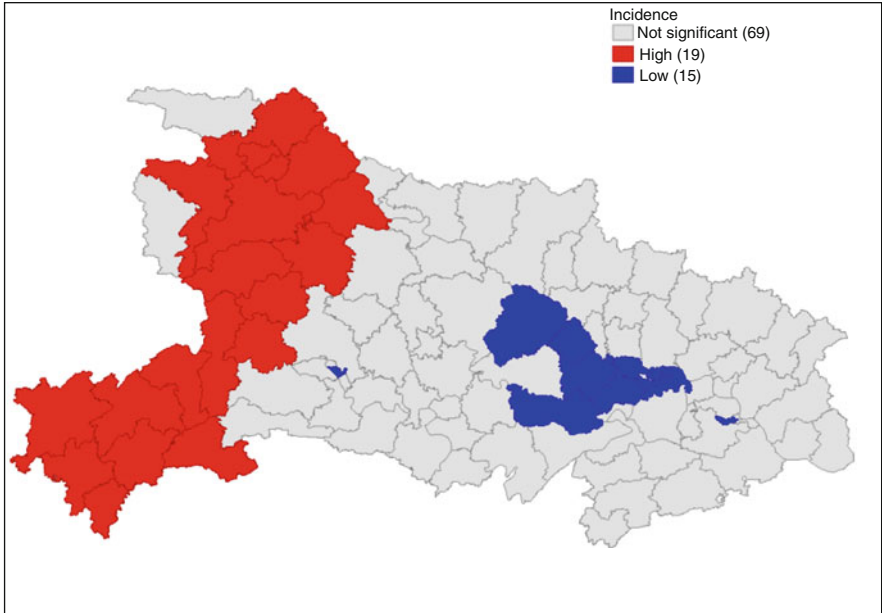


Fig. 6 Cluster map of poverty headcount ratio of Hubei province in 2013

elevation and slope are the most commonly used factors to describe the local terrain. The mean value and standard deviation of elevation and slope were adopted to describe the average level and dispersion degree of altitude and slope. Road density was chosen to indicate the overall transportation convenience and capacity in the region. Cropland is vital to the rural households for agriculture is the main mode of production in rural China. Furthermore, GDP per capita was selected to reflect the economic development and economic activity from statistic year book of Hubei province.

The correlation matrix of the correlation analysis suggests multicollinearity between variables with larger correlation coefficients. The step regression model was further employed to wipe out the collinearity problem between variables. Based on the results of step regression model, the variables mean elevation, GDP per capita and proportion of cropland were recognized for they made the most significant contribution to the regression model and are independent of each other. These three variables were entered into GWR model. The estimated results in the GWR models showed that the adjusted  $R^2$  of the model with the three variables is 0.71, which is higher than the value of 0.68 determined by the OLS model. The local  $R^2$  and explanatory variable coefficient of the variables in the GWR model were shown in Fig. 7.

The distribution of local  $R^2$  values presented great spatial variation, which implies the explanatory ability of the GWR model varies with county. Meanwhile,



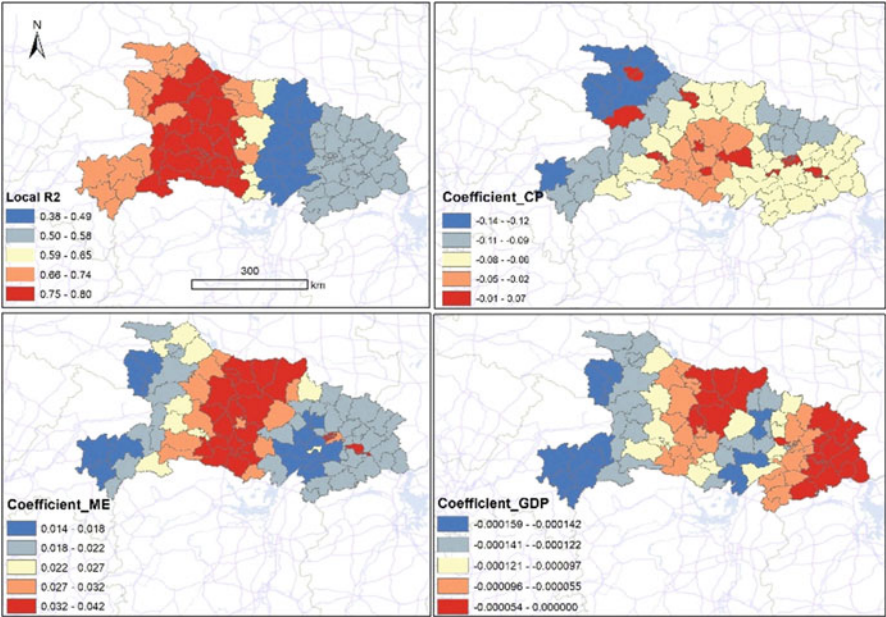


**Fig. 7** Local  $R^2$  and the three explanatory variable coefficients in GWR (CP means proportion of cropland in the total area of a region; ME means mean elevation)

the spatial distribution of each explanatory variable coefficients is similar but present different influence over space. Specifically, the mean elevation has a positive impact on the regional poverty, while GDP per capita and crop proportion have a negative impact, although the extent of this positive effect varies spatially. In addition, the spatial distribution of local  $R^2$  values and the coefficients of explanatory variables followed a similar characteristic of stratification that generally increased from east to west, implying the strength of the explanatory ability of the GWR model increases gradually from east to west.

**3.3 Spatial-Temporal Analysis: Case Study of an Alpine Area in China**

Ganzi Tibetan Autonomous Prefecture is a high poverty, alpine, ethnic, and ecologically protected area. This area plays an important role both in national ecological security and national harmony. Here we want to evaluate the living standard in Ganzi from the aspects of housing, infrastructure, medical care, social security, and education. Ten indicators were chosen to measure the living standard of Ganzi. Based on the collected socioeconomic data from Ganzi during the period of 2010–

2016, combined with the entropy weighting method and gray rational analysis, we evaluated the living standard in Ganzi from 2010 to 2016. Then, the spatial-temporal changes of evaluated living standard index of each county in Ganzi were investigated by using the Bayesian hierarchical model.

### 3.3.1 Study Area

Ganzi Tibetan Autonomous Prefecture, located in the plateau region of western Sichuan Province, which belongs to the Tibetan ethnic areas of Sichuan, Yunnan, Gansu, and Qinghai (Fig. 1). Ganzi, with 18 counties, is the largest Tibetan area in Sichuan Province and covers approximately 153 thousand km<sup>2</sup>. The highest altitude is 7556 m and the lowest is 1000 m. According to its geographical location, Ganzi was officially divided into three regions, northern, southern, and eastern Ganzi. Northern Ganzi has a higher altitude and harsher natural environment than the other two regions. Consequently, the socioeconomic conditions in northern Ganzi is quite lower than in eastern and southern Ganzi.

The high altitude leads to backward transportation and communication conditions in Ganzi. Furthermore, Ganzi is an ethnic minority area where Tibetan is dominant, accounting for 78.46% of the total population. Factors such as ideology, language barrier, and education level restrict poverty reduction and development. Moreover, Ganzi is located near the upper Yangtze river, which is also a water conservation area and plateau ecological barrier. Ganzi plays an important role both in national ecological security and national harmony. As an alpine area, ethnic area, and ecologically protected area, Ganzi faces serious challenges in poverty reduction and development. At the end of 2017, the poverty rate of Ganzi was 8.65%, the location of Ganzi is shown in Fig. 8.

### 3.3.2 Evaluation of Living Standard in Ganzi

The living standard evaluation includes ten indicators, as shown in Table 2. The chosen indicator categories were housing situation, infrastructure of rural village, medical care, social security, and education. Per capita living space was selected to reflect the housing situation. The population rate of tap water usage and the number of administrative villages that could be reached by road were used to measure the infrastructure. Medical technical personnel in health care institutions per 10,000 persons and the number of beds utilized in health care institutions per 10,000 persons were chosen to illustrate the medical care. New Rural Co-operative Medical System participants as a proportion of the total population was selected to represent the level of social security. The number of teachers per 10,000 persons and the ratio of expenditure on science and education to GDP indicated the education situation. The disposable income of rural households was chosen to reflect the income standard. Engel's coefficient was used to reflect the overall living condition

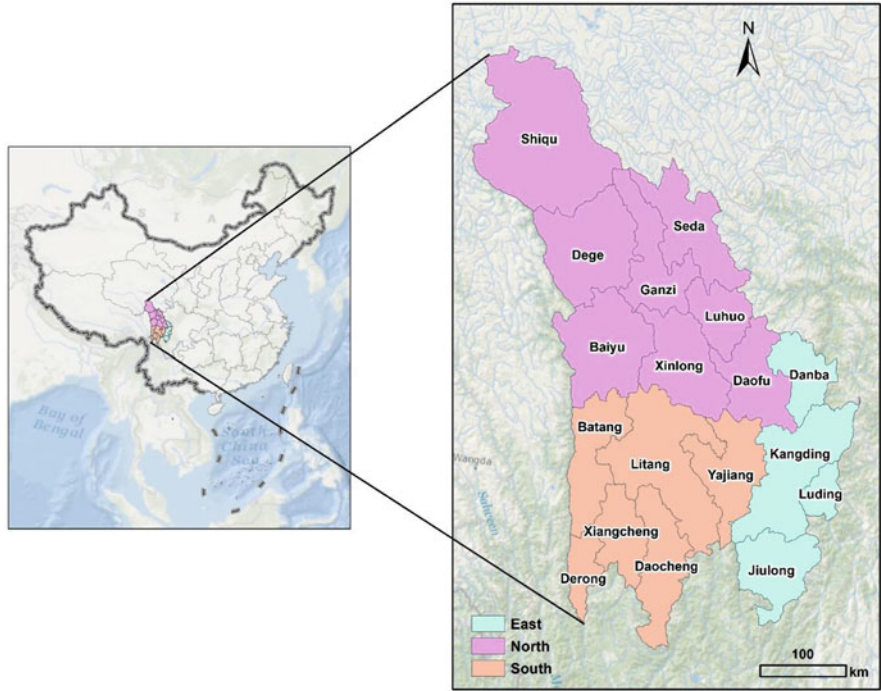


**Fig. 8** Location of Ganzi Tibetan autonomous prefecture

in poor areas. Moreover, Engel’s coefficient is a negative indicator in our evaluation index system, because the greater the value of Engel’s coefficient means the poorer the living standard of people.

The entropy weighting method was employed to define the weights for each evaluation indicator. After that, the Grey relational analysis was used to integrate various indicators into a comprehensive evaluation value to better assess the living standard in Ganzi from 2010 to 2016. Shannon’s entropy is widely used to determine weights, which is an objective method and determines weights only by data (Shannon 1984; Lotfi and Fallahnejad 2010). Here we used the entropy weighting method to determine the weights of each index. Gray system theory is proposed by Deng (1989). Grey relational analysis uses the order of Grey relational degrees to judge the strength or order of correlation between indicators and is widely applied for various evaluations (Tan and Deng 1995).

Supposing that there are  $m(m = 18)$  counties with  $n(n = 10)$  evaluated indicators, then the index system can be defined as:

$$X = \begin{bmatrix} x_{11} & \cdots & x_{1n} \\ \vdots & \ddots & \vdots \\ x_{m1} & \cdots & x_{mn} \end{bmatrix} \quad (3-1)$$

A standardization method was adopted to transform different value scales of indicator  $j$  into common measurable units by using:

$$y_{.j} = \frac{x_{.j} - \min(x_{.j})}{\max(x_{.j}) - \min(x_{.j})} \quad (3-2)$$

The information entropy of indicator  $j$  can be obtained by:

$$E_j = -\ln(n)^{-1} \sum_{i=1}^n \rho_{ij} \ln \rho_{ij} \quad (3-3)$$

$$\rho_{ij} = y_{ij} / \sum_{i=1}^n y_{ij} \quad (3-4)$$

Let  $\lim_{\rho_{ij} \rightarrow 0} \rho_{ij} \ln \rho_{ij} = 0$ , the weight of  $j$  can be obtained by:

$$w_j = \frac{1 - E_j}{n - \sum E_j} \quad (j = 1, 2, \dots, n) \quad (3-5)$$

Then, gray rational analysis was employed to obtain the evaluation index of living standard. First, we needed to normalize each indicator. For positive indicator  $j$ :

$$c_{ij} = \begin{cases} 1, & x_{ij} > S_j \\ \frac{x_{ij}}{S_j}, & x_{ij} \leq S_j \end{cases} \quad (3-6)$$

For positive indicator  $j$ :

$$c_{ij} = \begin{cases} 1, & x_{ij} \leq S_j \\ \frac{x_{ij}}{S_j}, & x_{ij} > S_j \end{cases} \quad (3-7)$$

where  $S_j$  is the reference value for indicator  $j$ , as shown in Table 4. The normalized indicator matrix  $C = [c_{i1}, c_{i2}, \dots, c_{in}]$ . Based on gray system theory, a standardization process is implemented on the normalized matrix to get the referential vector of indicators as  $c^* = [c_1^*, c_2^*, \dots, c_n^*]$ . Then, the relational coefficient of indicator  $j$  for county  $i$  can be calculated by:

**Table 4** Evaluation index framework of living standard in Ganzi

Project	Indicators	Reference value
Assessment of living standard in Ganzi Tibetan autonomous prefecture	Teachers per 10,000 persons <sup>a</sup>	100
	Medical technical personnel in health care institutions per 10,000 persons <sup>a</sup>	60
	Number of beds utilized in health care institutions per 10,000 persons <sup>a</sup>	50
	Engel's coefficient (%) <sup>a</sup>	40
	Popularization rate of tap water (%) <sup>a</sup>	100
	Ratio of administrative villages that can be reached by road (%) <sup>a</sup>	100
	Per-capita living space (m <sup>2</sup> per capita) <sup>a</sup>	30
	New Rural Co-operative Medical System participants as a proportion of total population (%)	100
	Ratio of expenditure on science and education to GDP (%) <sup>a</sup>	6
	Disposable income of rural household (yuan) <sup>b</sup>	8000

<sup>a</sup>National standard

<sup>b</sup>Local standard

$$\xi_{ij} = \frac{\min_i \max_j |c_j^* - c_{ij}| + \partial \max_i \min_j |c_j^* - c_{ij}|}{|c_j^* - c_{ij}| + \partial \max_i \max_j |c_j^* - c_{ij}|}$$

(3-8)

where  $\partial \in (0, \infty)$  is a predefined coefficient, set to 0.5. Finally, the evaluated living standard values can be calculated by:

$$R_i = \sum_{j=1}^n w_j * \xi_{ij}$$

(3-9)

Then the evaluation values were divided into five levels and labeled I to V to indicate the living standard in Ganzi from low to high, for each year.

The living standard in Ganzi improved remarkably, with an average growth rate of 24.72% from 2010 to 2016. As seen in Fig. 9, all the living standard evaluation indicators increased from 2010 to 2016. The disposable income of rural households was the major contributor to social condition growth, which was about 2.5 times higher in 2016 than it was in 2010. The housing, medical care, and educational conditions in Ganzi all saw significant improvement. The continuous improvement of social conditions from 2010 to 2016 in Ganzi can also be observed in Fig. 10.

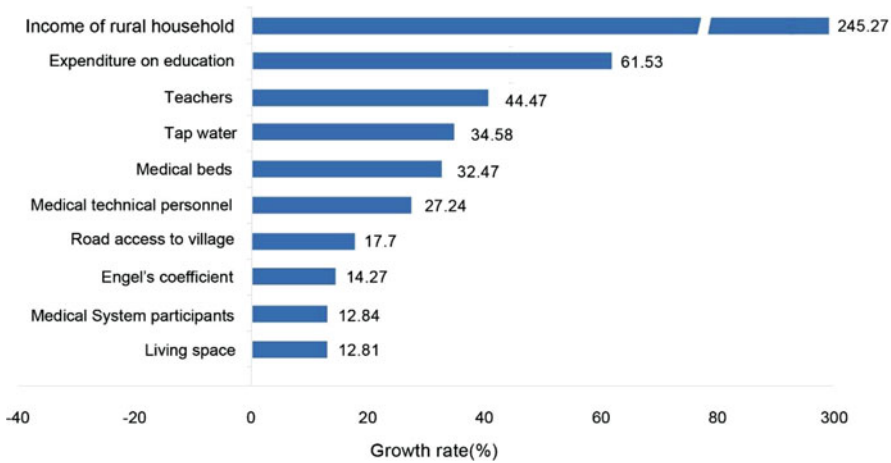


Fig. 9 Growth rate of evaluation indicators from 2010 to 2016 in Ganzi

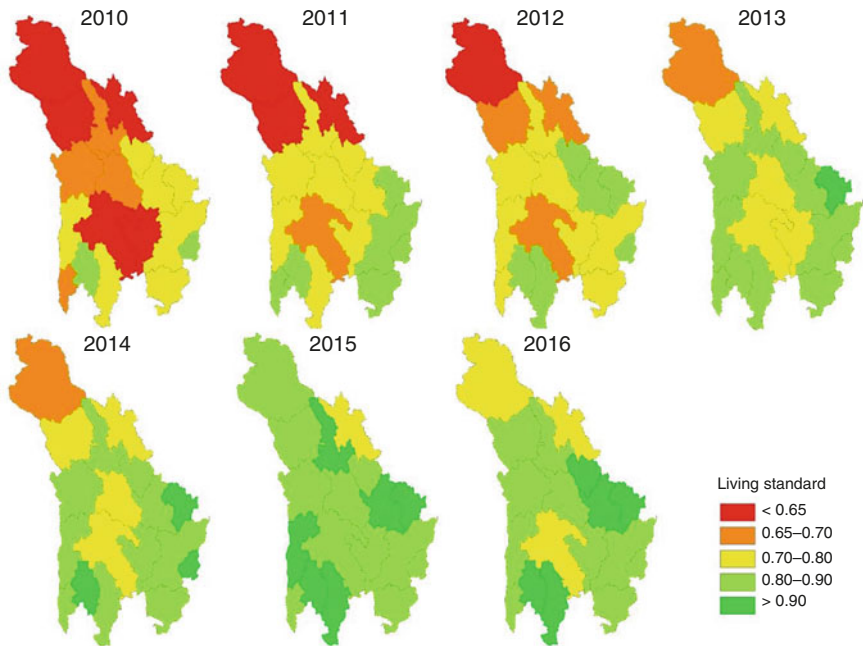


Fig. 10 Living standard evaluation index, categorized in five levels from 2010 to 2016 for Ganzi

The living standard also presented a regional difference, with higher living standard in eastern and southern Ganzi, and lower living standard in the northern region.

### 3.3.3 Spatial-Temporal Changes of Living Standard in Ganzi

The Bayesian hierarchical model was employed to explore the spatial-temporal pattern of the living standard in Ganzi from 2010 to 2016. The Bayesian hierarchical model was implemented using a statistical software named Open BUGS (Bayesian Inference Using Gibbs Sampling).

Based on the obtained living standard evaluation values, we investigated the spatial-temporal change pattern of the living standard in Ganzi. We denoted that  $y_{it}$  represents the evaluation value of  $i$ th ( $i = 1, 2, \dots, 18$ ) county at  $t$ th ( $t = -3, -2, -1, 0, 1, 2, 3$ ) year.

$$y_{it} \sim \text{Normal}(\mu_{it}, \sigma^2) \quad (3-10)$$

Thus, the  $\mu_{it}$  can be modeled as:

$$\log(\mu_{it}) = \alpha + S_i + b_0t + v_t + b_{1i}t + \varepsilon_{it} \quad (3-11)$$

where  $\alpha$  is the intercept term and assigned to follow a prior distribution of uniform distribution.  $S_i$  is the spatial term that describes the stable spatial pattern across the whole study area during the study period.  $b_0t + v_t$  describe the overall time trend pattern of the whole study area.  $b_{1i}t$  allows each county to have its own change trend.  $\varepsilon_{it}$  captures the additional variability in the data not explained by other model components. Prior distributions are needed to assigned for model parameters. The prior distributions of  $S_i$  and  $b_{1i}t$  are determined by the Besag York Mollie (BYM) model (Besag et al. 1991). In order to enhance the random effect of spatial structure in BYM, the conditional autoregressive (CAR) prior with a spatial adjacency matrix were employed at the same time (Li et al. 2014). The uniform distribution is assigned to  $b_0$  and  $\alpha$ . In addition,  $v_t$  is modeled as  $v_t \sim N(0, \sigma_v^2)$ , and  $\varepsilon_{it}$  is modeled as  $\varepsilon_{it} \sim N(\sigma_\varepsilon^2)$ . Both models were implemented using statistical software named OpenBUGS, which is specially designed for Bayesian analysis. Through Gibbs sampling and Metropolis algorithm, it could sample from complete conditional probability distribution and form MCMC chains, and finally estimating the parameters of the model through iteration (Lunn et al. 2000).

The obtained posterior median  $\exp(S_i)$  indicates the stable spatial component of the living standard from 2010 to 2016. The posterior of  $\exp(S_i)$  measured the living standard in  $i$ th county relative to the overall mean condition of the whole study area over the study period. The posterior median of  $\exp(S_i)$  more than 1 indicated a higher level than the overall condition, while less than 1 indicated a lower level than the overall condition. Figure 11a maps the posterior median of  $\exp(S_i)$ . There were 10 counties that had a higher level of living standard than the overall living standard in Ganzi, while 8 counties had a lower level of living standard. Luding County obtained the highest value of the posterior median of  $\exp(S_i)$  and Shiqu County obtained the lowest value. Furthermore, the distribution of the posterior median of



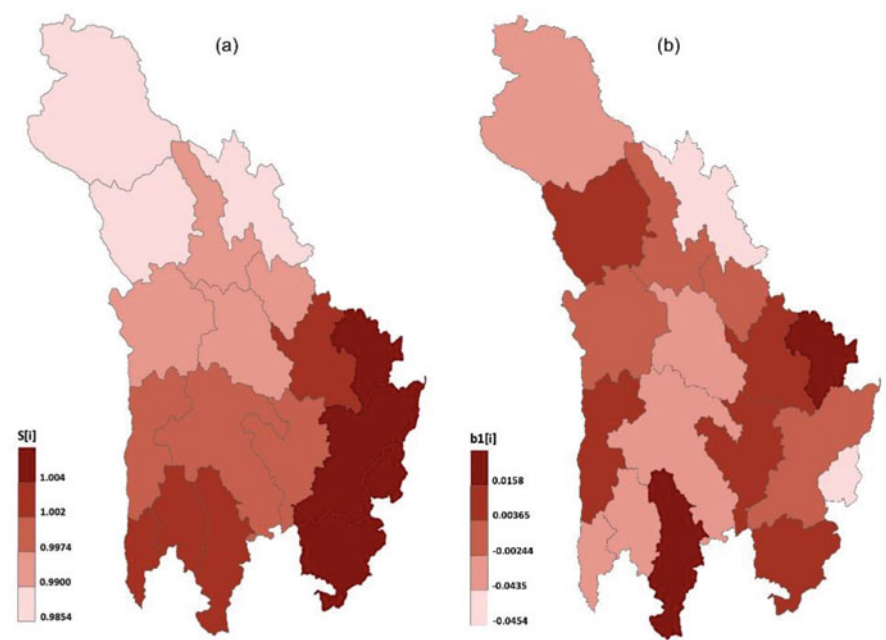


**Fig. 11** (a) The obtained posterior medians of  $(\exp(S_i))$  for living standard in each county of Ganzi (b) The deviations of the local trend to the overall trend  $(b_{1i})$  of living standard in each county of Ganzi

$\exp(S_i)$  presents an obvious regional disparity, with a high value concentrated in the eastern and southern regions and a low value concentrated in the northern region.

The obtained posterior median of  $b_{1i}$  measures the deviations of the local trend to the overall trend. A negative value of the posterior median of  $b_{1i}$  indicates that the speed of change of the evaluation index of  $i$ th county is slower than the overall change in Ganzi from 2010 to 2016. Conversely, a positive value of the posterior median of  $b_{1i}$  indicates that the speed of change of the evaluation index of  $i$ th county is more rapid than the overall change. Figure 11b maps the values of the posterior median of  $b_{1i}$ . Although the evaluation value of the living standard is quite low in northern Ganzi, such as Dege County and Ganzi County, they had more rapidly increased speed than the overall increase. Likewise, Luding County and Kangding County, located in eastern Ganzi, had the highest levels of living standard, but had a slower increase speed than the overall increase.

The obtained posterior median of  $\exp(b_0 + v_t)$  measures the overall temporal change trend of living standard in Ganzi from 2010 to 2016. Figure 12 plots the posterior median of  $\exp(b_0 + v_t)$  from 2010 to 2016. In Fig. 12, the living standard was continuously increasing from 2010 to 2016.



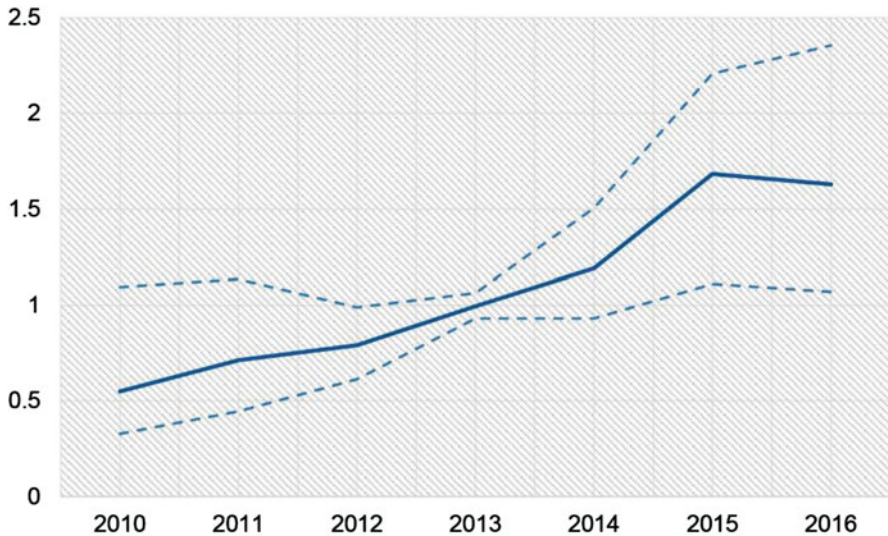


**Fig. 12** The temporal overall changing trend ( $\exp(b_0t + v)$ ) of living standard in Ganzi from 2010 to 2016

## References

- Alkire, S., & Fang, Y. (2018). Dynamics of multidimensional poverty and uni-dimensional income poverty: An evidence of stability analysis from China. *Social Indicators Research*, 142(1), 25–64.
- Alkire, S., & Foster, J. (2011). Counting and multidimensional poverty measurement. *Journal of Public Economics*, 95(7–8), 476–487.
- Anselin, L. (1995). Local indicators of spatial association-LISA. *Geographical Analysis*, 1(1), 1–24.
- Anselin, L. (2001). Spatial econometrics. In *A companion to theoretical econometrics* (pp. 311–330). Malden: Blackwell.
- Anselin, L. (2002). Under the hood Issues in the specification and interpretation of spatial regression models. *Agricultural Economics*, 27(2002), 247–267.
- Anselin, L., & Rey, S. (1991). Properties of tests for spatial dependence in linear regression models. *Geographical Analysis*, 23, 112–131.
- Atkinson, A. B. (1987). On the measurement of poverty. *Econometrica*, 55, 749–764.
- Besag, J., York, J., & Mollié, A. (1991). Bayesian image restoration, with two applications in spatial statistics. *Annals of the Institute of Statistical Mathematics*, 43(1), 1–20.
- Bird, K. (2019). *Addressing spatial poverty traps*. New York: United Nations.
- Chen, Y., & Ge, Y. (2015). Spatial point pattern analysis on the villages in China's poverty-stricken areas. *Procedia Environmental Sciences*, 27, 98–105.
- Cheng, X., Shuai, C., Wang, J., Li, W., Shuai, J., & Liu, Y. (2018). Building a sustainable development model for China's poverty-stricken reservoir regions based on system dynamics. *Journal of Cleaner Production*, 176, 535–554.
- Deller, S. (2010). Rural poverty, tourism and spatial heterogeneity. *Annals of Tourism Research*, 37(1), 180–205.
- Deng, J. L. (1989). Introduction to grey system theory. *Journal of Grey System*, 1(1), 1–24.

- Department of Household Surveys, National Bureau of Statistics of China. (2018). *Poverty monitoring report of China, 2018*. Beijing.
- Dollar, D. (2007). *Poverty, inequality and social disparities during China's economic reform*. The World Bank Policy Research Working Paper No. 4253, Washington, DC, 1–28.
- Ebdon, D. (1985). *Statistics in geography*. Oxford: Blackwell.
- Fotheringham, S., Brunsdon, C., & Charlton, M. (2002). *Geographically weighted regression: the analysis of spatially varying relationships*. Chichester: Wiley.
- Fotheringham, A. S., Crespo, R., & Yao, J. (2015). Geographical and temporal weighted regression (GTWR). *Geographical Analysis*, 1–22.
- Ge, Y., Yuan, Y., Hu, S., Ren, Z., & Yijin, W. (2017). Space–time variability analysis of poverty alleviation performance in China's poverty-stricken areas. *Spatial Statistics*, 21, 460–474.
- Getis, A. (1994). Spatial dependence and heterogeneity and proximal databases. In S. Fotheringham & P. Rogerson (Eds.), *Spatial analysis and GIS* (pp. 105–120). Oxford: Taylor and Francis.
- Haining, R. (1990). *Spatial data analysis in the social and environmental sciences*. Cambridge: Cambridge University Press.
- Information Office of the State Council. (2011). *New progress in development-oriented poverty reduction program for rural China*. Beijing.
- Jalan, J., & Ravallion, M. (1997). *Spatial poverty traps? The World Bank* (Policy Research Working Paper No. 1862). Washington, DC.
- Li, G., et al. (2014). Space–time variability in burglary risk: A Bayesian spatio-temporal modelling approach. *Spatial Statistics*, 9, 180–191.
- Li, Y., Long, H., & Liu, Y. (2015). Spatio-temporal pattern of China's rural development: A rurality index perspective. *Journal of Rural Studies*, 38, 12–26.
- Li, Y., Su, B., & Liu, Y. (2016). Realizing targeted poverty alleviation in China. *China Agricultural Economic Review*, 8(3), 443–454.
- Liu, Y. S., & Li, J. (2017). Geographic detection and optimizing decision of the differentiation mechanism of rural poverty in China. *Acta Geographica Sinica*, 72(1), 161–173.
- Liu, Y., & Xu, Y. (2016). A geographic identification of multidimensional poverty in rural China under the framework of sustainable livelihoods analysis. *Applied Geography*, 73, 62–76.
- Liu, Y., Liu, J., & Zhou, Y. (2017). Spatio-temporal patterns of rural poverty in China and targeted poverty alleviation strategies. *Journal of Rural Studies*, 52, 66–75.
- Liu, Y., Guo, Y., & Zhou, Y. (2018). Poverty alleviation in rural China: Policy changes, future challenges and policy implications. *China Agricultural Economic Review*, 10(2), 241–259.
- Lotfi, F. H., & Fallahnejad, R. (2010). Imprecise Shannon's entropy and multi attribute decision making. *Entropy*, 12(1), 53–62.
- Lunn, D. J., Thomas, A., Best, N., & Spiegelhalter, D. (2000). WinBUGS—A Bayesian modelling framework: Concepts, structure, and extensibility. *Statistics and Computing*, 10, 325–337.
- National Bureau of Statistics. (2019). *Statistical bulletin of the People's Republic of China on national economic and social development in 2018*. Beijing.
- Okwia, P. O., Ndeng'e, G., Kristjanson, P., Arunga, M., Notenbaert, A., Omolo, A., Henninger, N., Benson, T., Kariuki, P., & Owuor, J. (2007). Spatial determinants of poverty in rural Kenya. *PNAS*, 104(43), 16769–16774.
- Ouyang, Z. Y., Zheng, H., Xiao, Y., Polasky, S., Liu, J., Xu, W., et al. (2016). Improvements in ecosystem services from investments in natural capital. *Science*, 352(6292), 229–251.
- Paul Elhorst, J. (2014). *Spatial econometrics: From cross-sectional data to spatial panels*. Berlin Heidelberg: Springer.
- Ren, Z., Ge, Y., Wang, J., Mao, J., Zhang, Q., et al. (2017). Understanding the inconsistent relationships between socioeconomic factors and poverty incidence across contiguous poverty-stricken regions in China: Multilevel modelling. *Spatial Statistics*, 21, 406–420.
- Ripley, B. D. (1977). Modelling spatial patterns. *Journal of Royal Statistical Society*, 39, 172–212.
- Satya, R., & Chakravarty, C. D. A. (2006). The measurement of social exclusion. *Review of Income and Wealth*, 52, 377–398.
- Sen, A. K. (1976). Poverty: An ordinal approach to measurement. *Econometrica*, 44, 219–231.

- Sen, A. K. (2001). *Development as freedom* (2nd ed.). Oxford New York: Oxford University Press.
- Shannon, C. E. (1984). *A mathematical theory of communication* (Vol. 27, pp. 379–423). Urbana: University of Illinois Press.
- Sparks, C., & Campbell, J. (2013). An application of Bayesian methods to small area poverty rate estimates. *Population Research and Policy Review*, 33(3), 455–477.
- Sparks, C., & Campbell, J. (2014). An application of Bayesian methods to small area poverty rate estimates. *Population Research and Policy Review*, 33(3), 455–477.
- Tan, X. R., & Deng, J. L. (1995). *Grey relational analysis: A new method of multi factors statistical*. *Statistical Research*, 3, 46–48.
- The State Council. (2011). *The outline for development-oriented poverty reduction for China's rural area (2011–2020)*. Beijing: State Council.
- The World Bank. (2018). *Poverty and shared prosperity 2018: Piecing together the poverty puzzle*. Washington, DC: World Bank.
- Tu, J., & Xia, Z. G. (2008). Examining spatially varying relationships between land use and water quality using geographically weighted regression I: Model design and evaluation. *Science of the Total Environment*, 407(1), 358–378.
- UNDP. (2010). *Human development report 2010: The real wealth of nations: Pathways to human development*. New York: Palgrave Macmillan.
- United Nations. (2015a). *Transforming our world: the 2030 agenda for sustainable development*. New York: United Nations.
- United Nations. (2015b). *The millennium development goals report*. New York: United Nations.
- Wang, X. (2012). Poverty criteria and global poverty situation. *Review of Economic Research*, 55, 41–50.
- Wang, J. F., et al. (2010). Geographical detectors-based health risk assessment and its application in the neural tube defects study of the Heshun Region, China. *International Journal of Geographical Information Science*, 24(1), 107–127.
- Wang, X. L., Wang, L. M., & Wang, Y. (2014). *The quality of growth and poverty reduction in China*. Berlin: Springer.
- Wang, J. F., Zhang, T. L., & Fu, B. J. (2016). A measure of spatial stratified heterogeneity. *Ecological Indicators*, 67, 250–256.
- Watmough, G. R., et al. (2019). Socioecologically informed use of remote sensing data to predict rural household poverty. *Proceedings of the National Academy of Sciences of the United States of America*, 116(4), 1213–1218.
- Xu, W., et al. (2017). Strengthening protected areas for biodiversity and ecosystem services in China. *Proceedings of the National Academy of Sciences of the United States of America*, 114(7), 1601–1606.
- Zhang, C., Tang, Y., Xu, X., & Kiely, G. (2011). Towards spatial geochemical modelling: use of geographically weighted regression for mapping soil organic carbon contents in Ireland. *Applied Geochemistry*, 26(7), 1239–1248.
- Zhang, C., et al. (2014). Are poverty rates underestimated in China? New evidence from four recent surveys. *China Economic Review*, 31, 410–425.
- Zhou, Y., & Liu, Y. (2019). The geography of poverty: Review and research prospects. *Journal of Rural Studies*. <https://doi.org/10.1016/j.jrurstud.2019.01.008>.
- Zhou, Y., Guo, Y., Liu, Y., Wu, W., & Li, Y. (2018). Targeted poverty alleviation and land policy innovation: Some practice and policy implications from China. *Land Use Policy*, 74, 53–65.
- Zuo, C. S. (2016). *Evolution of China's poverty alleviation and development policy (2001–2015)* (pp. 16–18, 73). Beijing: Social Science Academic Press.